

Investigation of optimization Algorithms and Their Operating Parameters in Different Types of Heat Exchangers

Authors

Mohsen Hajabdollahi ^a
Mohammad Shafiey Dehaj ^{b*}
Hassan Hajabdollahi ^b

^a Department of Computer Engineering,
Vali-e-Asr University of Rafsanjan,
Rafsanjan, Iran

^b Department of Mechanical
Engineering, Vali-e-Asr University of
Rafsanjan, Rafsanjan, Iran

ABSTRACT

In this study, five different heat exchangers (HE) including, plate-fin (PFHE), fin tube (FTHE), rotary regenerator (RR), shell and tube (STHE) and gasket plate (GPHE) are optimized using four different algorithms including the binary genetic algorithm (BGA), real parameter genetic algorithm (RGA), particle swarm optimization (PSO) algorithm and the differential evolution (DE) algorithm. Verified codes are used for all heat exchangers and total annual cost (TAC) is considered as the objective function and heat exchanger configuration parameters are chosen as design parameters in all studied exchangers. RGA has the lowest insensitivity to the algorithm input parameters, or lowest relative standard deviation (RSD), for all studied heat exchangers. The best TAC in the GPHE, FTHE, PFHE, RR, STHE can be achieved in the points $\langle C_1, C_2 \rangle = (0, 0.6), (0, 1.95), (0, 1.5), (0, 2.1), (0, 1.65)$ and $\langle \eta_c, \eta_m \rangle = (2.4, 2.4), (1, 2.4), (3.25, 3.75), (3.15, 3), (2.6, 2.8)$ where the lowest run-time and RSD are our basic requirements, respectively. The results also reveal that DE has the worst result in the case of RSD and GA has the worst result in the case of run-time. Finally, RGA is recommended for the optimization of different types of heat exchangers.

Article history:

Received : 13 February 2021

Accepted : 11 August 2021

Keywords: Different Types of Heat Exchangers; Optimization Algorithms; Objective Function; Algorithm Operating Parameters.

1. Introduction

There are a lot of efforts for optimization of different types of heat exchangers with various objectives and various methods. In recent years, Hajabdollahi et al. performed the optimization of different types of heat exchangers including the shell and tube [3-5], condenser [4], plate-fin [5-7], fin tube [8-9], rotary regenerator [10] as well as gasket plate [11] by using different algorithms including Genetic Algorithm [1-4, 4-

11], Particle Swarm Algorithm [4], Firefly Algorithm [3] and by considering the different objective functions including total annual cost [1-6, 8-9, 11], effectiveness [2-3, 5, 8-9, 10-11], pressure drop [7, 10], exergy efficiency [1, 6], entropy generation [6] and temperature approach [9]. The use of genetic and particle swarm algorithms in the design of shell-and-tube, plate-fin, fin-tube and regenerator heat exchangers was demonstrated by many authors.

Techno-economic optimization of a shell and tube heat exchanger by genetic and particle swarm algorithms was performed by Sadeghzadeh et al [12]. Results showed that results obtained with the particle swarm optimization method were superior to those

*Corresponding author: Mohammad Shafiey Dehaj,
Department of Mechanical Engineering, Vali-e-Asr
University of Rafsanjan
Email address: m.shafiey@vru.ac.ir

obtained with the genetic algorithm method. Also, Sadeghzadeh et al. presented an optimization of a finned shell and tube heat exchanger using a multi-objective genetic algorithm to obtain the maximum heat transfer rate and minimum cost [13]. In new research, Hajabdollahi presented the thermoeconomic optimization of plate-fin heat exchangers with similar (SF) and different (DF) or non-similar fin on each side [15]. For this purpose, both heat exchanger effectiveness and total annual cost (TAC) are optimized simultaneously using a multi-objective particle swarm optimization algorithm. Results displayed for the thermodynamic optimization viewpoint both SF and DF had the same optimum result while for the economic (or thermoeconomic) optimization viewpoint, the significant decrease in TAC was accessible in the case of DF compared with SF.

In another research, Emrah Turgut investigated the utilization of the Hybrid Chaotic Quantum behaved Particle Swarm Optimization (HCQPSO) algorithm for the thermal design of plate-fin heat exchangers [16]. It was observed that the proposed algorithm successfully converged to optimum configuration with higher accuracy. Further to the previous studies the thermal design of shell and tube heat exchangers to investigate the economic design and thermal performance was conducted by Turgut et al [17]. It was concluded that the performance of MPFHE with regards to heat transfer and fluid flow was effectively improved by the optimization design of the genetic algorithm (GA) layer pattern. In another new study, Wang and Li introduced and applied an improved multi-objective cuckoo search (IMOCS) algorithm for the multi-objective optimization design of plate-fin heat exchangers (PFHEs) [18]. It was demonstrated that the presented method was able to obtain optimum solutions with higher accuracy, lower irreversibility, and fewer iterations as compared to the single-objective design approaches.

In several research analyses for chevron-type plate heat exchangers, various algorithms have been utilized to examine the effects of different parameters. The characteristics of pressure drop and heat transfer for chevron-type plate heat exchangers were investigated

by Lee and Soo Lee [19]. Design optimization was also conducted by using the micro-genetic algorithm and considering the JF factor as an objective function. The optimal points ($\beta = 66.5^\circ$ and $p/h = 2.73$) were almost constant, regardless of the Reynolds number. Arie et al. focused on the numerical modeling and optimization of a manifold-microchannel plate heat exchanger to determine the design parameters that gave the optimum performance for the heat exchanger [20]. The optimized manifold-microchannel plate heat exchanger showed superior heat transfer performance over chevron plate heat exchanger designs. The effects of different parameters used in the design of the fin-tube heat exchanger by different algorithms were considered by some researchers. Hong et al. presented a numerical analysis of the performance of a fin-tube type adsorption chiller associated with heat and mass transfer mechanisms [21]. The result showed that fin thickness and the temperature of hot water were the dominant parameters for COP and SCP, respectively.

Kubo et al. [22] suggested an optimal design procedure for plate-type microchannel reactor manifolds, by a level set-based topology optimization procedure that objectives flow uniformity in the microchannels. They presented two-dimensional Z-kind and U-kind manifold design problems in numerical cases to prove the utility of their suggested procedure. Ramalingom et al. [23] performed a multi-objective topology optimization problem in an asymmetrically heated channel, to minimize the pressure drop and maximize the heat transfer. The results showed that the thermal exchanges were enhanced by calculating the Nusselt numbers and bulk temperature. Wang et al. [24] suggested the optimal design of a HEN that attempts to optimize separately the integer and continuous variables on two levels. Two levels included a problem-oriented evolution procedure and a memetic particle swarm optimization.

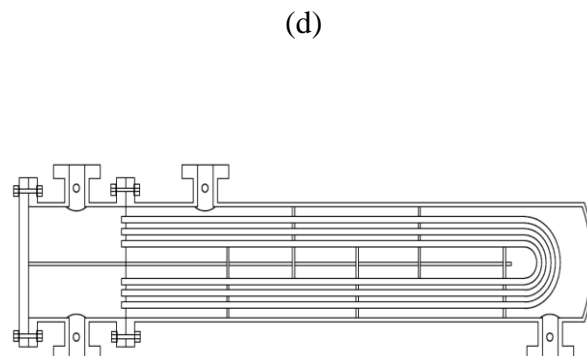
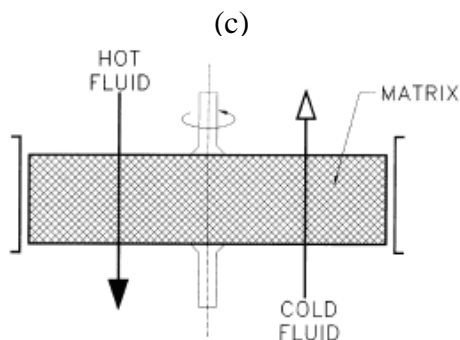
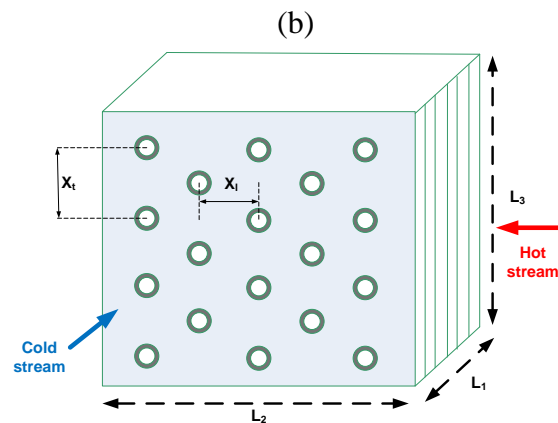
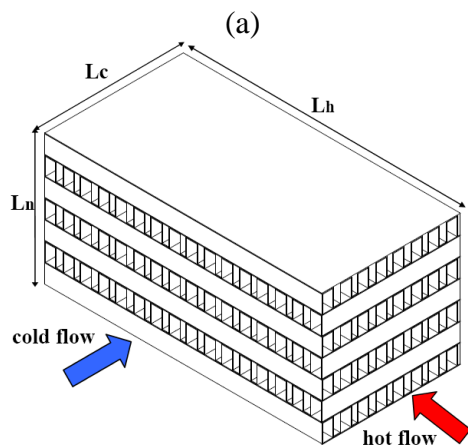
Hajabdollahi et al. [25] and Ahmadi et al. [26] carried out a comprehensive thermal modeling and optimal design of a PTHE and compact HE by employing epsilon-NTU procedure for estimation of pressure drop and effectiveness, respectively. They provided the

results of optimal designs in a set of multiple optimum solutions, called Pareto-optimal solutions. Additionally, a sensitivity analysis of change in optimum effectiveness and TAC with changes in design parameters of the heat exchangers is also carried out in detail. A thermoeconomic optimization of a shell and tube condenser, based on two new optimization procedures, namely genetic and particle swarm (PS) algorithms performed by Hajabdollahi et al. [27]. Results indicated that an enhancement in the tube number leads to reduce in the objective function first then it leads to a considerable increment in the objective function.

In the mentioned works, many populations based algorithms were used for the optimization of different types of heat exchangers. However, the performance and advantage of different optimization algorithms for different heat exchangers are not investigated. In fact, it is not clear for the researcher which algorithm is more

efficient for optimization of heat exchangers from different points of view including convergence and running time. In addition, the suitable trend and range of controlling parameters in each optimization algorithm are not investigated.

In this study, five different heat exchangers including, a plate-fin heat exchanger (PFHE), fin tube heat exchanger (FTHE), rotary regenerator (RR), shell and tube heat exchanger (STHE) and gasket plate heat exchanger (GPHE) shown in Fig. 1 are optimized using four different algorithms including the binary genetic algorithm (BGA or GA), real parameter genetic algorithm (RGA), particle swarm optimization (PSO) algorithm and the differential evolution (DE). The results are presented in the aspects of time-consuming and cost optimization, and the most practical algorithms for different heat exchangers are introduced.



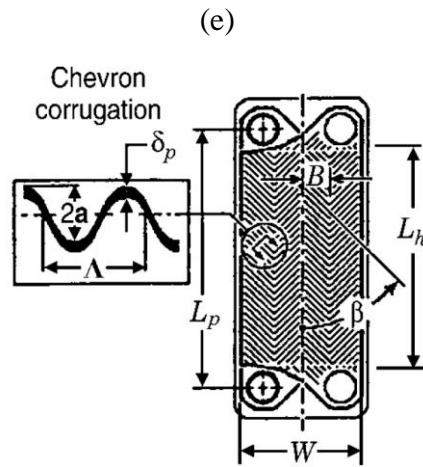


Fig. 1. Schematic diagram of five studied heat exchangers: a. plate-fin heat exchanger (PFHE), b. fin tube heat exchanger (FTHE), c. rotary regenerator (RR), d. shell and tube heat exchanger (STHE), e. gasket plate heat exchanger (GPHE)

Nomenclature

A_{tot}	total heat transfer area (m^2)	G	mass flux (kg/m^2s)
af	annualized factor (-)	h	heat transfer coefficient (W/m^2K)
b	fin height (m)	h_{id}	ideal heat transfer coefficient (W/m^2K)
c_p	specific heat (J/kgK)	H	enthalpy (W)
c	fin pitch (m)	i	interest rate (-)
C_1	Self-confidence factor in PSO	j	Colburn number (-)
C_2	Swarm-confidence factor in PSO	k_f	fin conductivity ($W/m.K$)
C_{min}	minimum of Ch and Cc (W/K)	k_w	wall conductivity ($W/m.K$)
C_{max}	maximum of Ch and Cc (W/K)	L	tube length (m)
C^*	heat capacity rate ratio (C_{min}/C_{max})	n_p	number of tube pass (-)
C_{in}	investment cost ($\$/year$)	N	operational hours in a year
C_{op}	operational cost ($\$/year$)	N_r	number of tube row (-)
C_r	Crossover rate in DE	N_t	number of tubes (-)
d_i	tube inside diameter (m)	NTU	number of transfer units (-)
d_o	tube outside diameter (m)	P_c	Probability of crossover in GA
d_c	fin collar outside diameter (m)	p_f	fin pitch (m)
D_h	hydraulic diameter (m)	P_m	Probability of mutation in GA
f	friction factor (-)	Pr	Prandtl number (-)
F	Differential weight in DE	R_f	fouling resistance (m^2K/W)
		R_w	wall resistance (m^2K/W)
		Re	The Reynolds number (-)
		S_{C_1}	the step size of C_1 in PSO

S_{C2}	the step size of C_2 in PSO
S_{Cr}	the step size of Cr in DE
S_F	the step size of F in DE
S_{pc}	the step size of Pc GA
S_{pm}	the step size of Pm in GA
S_{η_c}	the Step size of η_c RGA
S_{η_M}	the Step size of η_M in RGA
St	the Stanton number (-)
TAC	total annual cost(\$/year)
t	wall thickness (m)
t_f	fin thickness (m)
U	the overall heat transfer coefficient (W/m^2K)
x	fin length (m)
X_l	longitudinal pitch (m)
X_t	transversal pitch (m)
y	lifetime (year)

Greek abbreviation

ε	heat exchanger effectiveness (-)
η	compressor or fin efficiency (-)
η_c	Crossover parameter in RGA
η_M	Mutation parameter in RGA
β	corrugation angle (degree)
μ	viscosity (Pa.s)
ΔP	pressure drop (Pa)
φ_e	the unit price of electrical (\$MWh ⁻¹)

Subscripts

c	Cold
h	hot

2. Thermal modeling

In heat exchangers, there are usually no external heat and work interactions, and the first law of thermodynamic in steady-state yields

$$\Delta H_c = \Delta H_h, \tag{1}$$

where subscripts c and h represent the cold and hot stream. In this study, the effectiveness-

NTU (number of transfer unit) method is used to estimate the heat exchanger thermal performance for all studied heat exchangers. The best heat exchanger flow arrangement is counter flow with the highest effectiveness. RR and GPHE have the counter-flow arrangement while PFHE and FTHE have the cross-flow arrangement (because of manufacturing difficulties with counter-flow arrangement) and STHE has the mixed flow arrangement between the mentioned arrangements.

The effectiveness of counter flow heat exchanger, cross-flow arrangement with both fluids unmixed and E type TEMA shell and tube heat exchanger are, respectively, estimated as [28]

$$\varepsilon = \frac{1 - e^{-NTU(1-C^*)}}{1 - C^* e^{-NTU(1-C^*)}}, \tag{2}$$

$$\varepsilon = \frac{2}{(1 + C^*) + (1 + C^{*2})^{0.5} \coth(\frac{NTU}{2}(1 + C^{*2})^{0.5})}, \tag{3}$$

and

$$\varepsilon = 1 - \exp\left\{(1/C^*)NTU^{0.22} \times (\exp\{-C^*(NTU)^{0.78}\} - 1)\right\} \tag{4}$$

in which C^* and NTU are the number of transfer units and total heat capacity ratio defined as [22]

$$NTU = \frac{(UA_{tot})_h}{C_{min}} = \frac{(UA_{tot})_c}{C_{min}} \text{ and} \tag{5}$$

$$C^* = C_{min} / C_{max}, \tag{6}$$

where A_{tot} is total heat transfer area, U is the overall heat transfer coefficient, and subscripts c and h respectively refer to the cold and hot side. The overall heat transfer coefficient is a function of convection heat transfer resistance in each side (cold and hot), fouling resistance, as well as wall conduction heat transfer resistance. That is,

$$(UA_{tot})_h = (UA_{tot})_c = \frac{1}{\frac{1}{\eta_h h A_{tot,h}} + \frac{R_{f,h}}{\eta_h A_{tot,h}} + R_w + \frac{R_{f,c}}{\eta_c A_{tot,c}} + \frac{1}{\eta_c h A_{tot,c}}} \tag{7}$$

where η is overall fins efficiency. Usually, the fin (and thus the fin efficiency) is used for the side with a low convection heat transfer coefficient or for a heat exchanger with gas as hot/cold fluid. In this study, fins are used for both sides of PFHE and the gas side of FTHE. R_f is fouling resistances which is usually negligible for the air as the working fluid. In

addition, R_w is wall conduction heat transfer resistance which is usually negligible for PFHE (because a very thin plate is used between the fins on each side, and as a result, the conduction resistance is negligible compared with the convection resistance). Wall conduction heat transfer resistance for a flat plate surface such as GPHE is computed as [28]

$$R_w = \frac{t}{k_w A_{tot}}, \quad (8)$$

and for a tubular heat transfer wall such as STHE and FTHE this value is computed as [28]

$$R_w = \frac{\ln(d_o / d_i)}{2\pi k_w L}, \quad (9)$$

where t , k_w , L , d_o and d_i are wall thickness, wall conductivity, tube length, outer and inner tube diameters, respectively.

$$j = 0.6522(\text{Re})^{-0.5403}(\alpha)^{-0.1541}(\delta)^{0.1499}(\gamma)^{-0.0678} \times [1 + 5.269 \times 10^{-5}(\text{Re})^{1.34}(\alpha)^{0.504}(\delta)^{0.456}(\gamma)^{-1.055}]^{0.1} \quad \text{and} \quad (12)$$

$$f = 9.6243(\text{Re})^{-0.7422}(\alpha)^{-0.1856}(\delta)^{0.3053}(\gamma)^{-0.2659} \times [1 + 7.669 \times 10^{-8}(\text{Re})^{4.429}(\alpha)^{0.920}(\delta)^{3.767}(\gamma)^{0.236}]^{0.1} \quad (13)$$

are used [29]. The above correlations are accurate within $\pm 20\%$ and are valid for $120 < \text{Re} < 10^4$, $0.134 < \alpha < 0.997$, $0.012 < \delta < 0.048$ and $0.041 < \gamma < 0.121$, where

$$\alpha = c/b \quad \delta = t_f/x \quad \gamma = t_f/c, \quad (14\text{-a-c})$$

where c , b , t_f , x are fin pitch, fin height, fin thickness and fin length, respectively. In addition, Re is the Reynolds number, which is

$$j = \begin{cases} 0.108 \text{Re}_{dc}^{-0.29} (X_t / X_l)^{c_1} (p_f / d_c)^{-1.084} (p_f / D_h)^{-0.786} (p_f / X_t)^{c_2} & \text{for } N_r = 1 \\ 0.086 \text{Re}_{dc}^{c_3} . N_r^{c_4} (p_f / d_c)^{c_5} (p_f / D_h)^{c_6} (p_f / X_t)^{-0.93} & \text{for } N_r \geq 2 \end{cases} \quad (16)$$

and

$$f = 0.0267 \text{Re}_{dc}^{c_7} (X_t / X_l)^{c_8} (p_f / d_c)^{c_9} \quad (17)$$

where c_1 to c_9 are some simplified parameters that are available in reference [30].

The above equations are valid for $6.9 \leq d_c \leq 13.6 \text{ mm}$ and for $300 < \text{Re} < 20000$, $20.4 \leq X_t \leq 31.8 \text{ mm}$, $1.3 \leq D_h \leq 9.37 \text{ mm}$

2.1. Convection heat transfer coefficient for the gas side of PFHE, RR and FTHE

Convection heat transfer coefficient for both sides of PFHE, both side of RR and fin side of FTHE is calculated from [28]

$$h = St G c_p, \quad (10)$$

where G is the mass flux, and St is the Stanton number defined as

$$St = j / \text{Pr}^{2/3}, \quad (11)$$

in which Pr is the Prandtl number and j is the Colburn factor. Colburn and Fanning friction factor correlations on both sides of PFHE, both sides of RR, and the fin side of FTHE is estimated in the next subsections.

2.1.1. Colburn and Fanning friction factor correlations for both sides of PFHE

In this study rectangular offset strip fin with the following Colburn and Fanning friction factor correlations defined as

a function of the mass flux, hydraulic diameter and viscosity, is defined as

$$\text{Re} = D_h G / \mu \quad (15)$$

2.1.2. Colburn and Fanning friction factor correlations for fin side of FTHE

The Colburn and Fanning friction factors for plain flat fins on staggered tube banks are given as [30]

and $1.0 \leq p_f \leq 8.7 \text{ mm}$, $12.7 \leq X_t \leq 32 \text{ mm}$ relations for The proposed co. $1 \leq N_r \leq 6$ Colburn number and f factor, are accurate within $\pm 15\%$ [24].

The Reynolds number and the hydraulic diameter are defined as [30]

$$Re_{dc} = Gd_c / \mu \quad (18)$$

where

$$d_c = d_o + 2\delta \quad (19)$$

and G is mass flux.

2.1.3. Colburn and Fanning friction factor correlations for both sides of RR

The following Colburn and Fanning friction factors for a randomly stacked woven-screen matrix are proposed in form of [10]:

$$j = a_1(Re)^{-a_2} + a_3 \quad (20)$$

$$f = 10^{g(\log(Re))} \quad (21)$$

$$g(x) = b_1x^3 + b_2x^2 + b_3x + b_4 \quad (22)$$

where Reynolds number has the same form with the case of PFHE and coefficients a and b are constants [10].

2.2. Convection heat transfer coefficient for tube side

Convection heat transfer coefficient in tube side of STHE and FTHE are estimated as f [31]

$$h = \frac{k_f}{d_i} \left(3.657 + \frac{0.0677 \cdot (Re \cdot Pr \cdot d_i / L)^{1.33}}{1 + 0.1 \cdot Pr(Re \cdot d_i / L)^{0.3}} \right) \quad (23)$$

for $Re \leq 2300$,

$$h = \frac{k_f}{d_i} \left\{ \frac{\frac{f}{2} \times (Re - 1000) \cdot Pr}{1 + 12.7 \cdot \sqrt{\frac{f}{2}} (Pr^{0.67} - 1)} \right\} \quad \text{for} \quad (24)$$

$2300 < Re \leq 10000$,

$$\text{and } f = (1.58 \log(Re) - 3.28)^{-2} \quad (25)$$

$$h = \frac{k_f}{d_i} \left\{ \frac{\frac{f}{2} \times Re \cdot Pr}{1.07 + \frac{900}{Re} - \frac{0.63}{1 + 10Pr} + 12.7 \cdot \sqrt{\frac{f}{2}} (Pr^{0.67} - 1)} \right\} \quad (26)$$

for $Re > 10000$

$$f = 0.00128 + 0.1143(Re)^{-0.311} \quad (27)$$

where f is the friction factor and Re is the Reynolds number defined as

$$Re = \frac{4\dot{m}_p}{\pi d_i \mu N_t}, \quad (28)$$

where n_p and N_t are respectively the number of tube passes and tube numbers.

2.3. Convection heat transfer coefficient for GPHE

Convection heat transfer coefficient and Fanning friction factor for both sides of GPHE which are chevron plate cores are proposed in form of [32]

$$h = (k / D_h) 0.205 Pr^{1/3} \left(\frac{\mu_m}{\mu_w} \right)^{1/6} (f \cdot Re^2 \sin 2\beta)^{0.374} \quad (29)$$

and

$$f = \frac{c_1}{Re^{c_2}} \quad (30)$$

where β is corrugation angle and c_1 and c_2 are constants [32]. The value of μ_m and μ_w (viscosity) should be obtained at the average temperature of the stream and the wall temperature, respectively.

2.4. Convection heat transfer coefficient for shell side of STHE

The Bell-Delaware method was used in this paper to compute the shell side heat transfer coefficient and pressure drop in form of [28]

$$h = h_{id} J_c J_l J_b J_s J_r, \quad (31)$$

where h_{id} is the heat transfer coefficient for the ideal exchanger with pure cross-flow stream over tube bundle evaluated at a Reynolds number at or near the centerline of the shell in form of [28]

$$h_{id} = j_s c_{p,s} \left(\frac{m_s}{A_s} \right) \left(\frac{k_s}{c_{p,s} \mu_s} \right)^{2/3} \left(\frac{\mu_s}{\mu_{s,w}} \right)^{0.14}, \quad (32)$$

where j_s is the ideal tube bank Colburn factor, A_s is the cross-flow area at or near the shell centerline and $\mu_s / \mu_{s,w}$ is the ratio of viscosity ratio at bulk to wall temperature in the shell side.

The total shell side pressure drop was computed as the sum of three terms including cross-flow pressure drop (Δp_{cr}), inlet and outlet pressure drop (Δp_{i-o}) and window section pressure drop (Δp_w) as [28]

$$\Delta p_s = \Delta p_{cr} + \Delta p_{i-o} + \Delta p_w, \quad (33)$$

Details of computing the Colburn factor, friction factor, overall heat transfer coefficient and pressure drop for different studied heat exchangers are given in reference [28].

3. Economic modeling

Total annual cost (TAC) is in terms of initial cost (annual cost of total heat transfer surface area) and operational cost for electricity consumption by compressor/pump to overcome the friction and is given as [2, 5, 6, 10-11]

$$TAC(\$/\text{year}) = afC_{in} + C_{op}, \quad (34)$$

$$C_{in} = d_1 + d_2 \times A_{tot}^{d_3} \quad \text{and} \quad (35)$$

$$C_{op} = \left\{ \left(\frac{\Delta PV}{\eta} \right)_c + \left(\frac{\Delta PV}{\eta} \right)_h \right\} \varphi_e N, \quad (36)$$

where C_{in} , C_{op} , η , V , φ_e , Δp and N are investment cost, operational cost, compressor efficiency, volume flow rate, electricity unit price, pressure drop and operation hours in a year, respectively. Furthermore, d_1 and d_2 are constants and af is the annual cost coefficient defined as

$$af = \frac{i}{1 - (1+i)^{-y}}, \quad (37)$$

where i and y are interest rate and lifetime, respectively.

4. Objective functions, design parameters and constraints

In this study, the total annual cost (TAC) for each studied heat exchanger is considered as the objective function.

4.1. Plate fin heat exchanger

In this study, six design parameters including fin pitch (c), fin height (b), fin offset length (x), and heat exchanger geometry, including cold stream flow length (L_c), no-flow length (L_n) and hot stream flow length (L_h) are selected. The constraints are also introduced to ensure that the α , δ and γ are in the range of $0.134 < \alpha < 0.997$, $0.012 < \delta < 0.048$ and $0.041 < \gamma < 0.121$ [5].

4.2. Fin tube heat exchanger

Eight design parameters including longitudinal pitch, transversal pitch, fin pitch, number of tube pass, tube diameter, cold stream flow length, no-flow length and hot stream flow length were selected. The constraints are introduced to ensure that the d_c , D_h , X_t , X_l , p_f and N_r are in the range of $6.9 \leq d_c \leq 13.6 \text{ mm}$, $1.3 \leq D_h \leq 9.37 \text{ mm}$, $20.4 \leq X_t \leq 31.8 \text{ mm}$, $12.7 \leq X_l \leq 32 \text{ mm}$, $1.0 \leq p_f \leq 8.7 \text{ mm}$ and $2 \leq N_r \leq 6$ [8].

4.3. Rotary regenerator

Six design parameters including frontal area, the ratio of hot to cold frontal, matrix thickness, matrix rotational speed, matrix rod diameter and porosity are selected for optimization of RR [10].

4.4. Shell and tube heat exchanger

Seven design parameters including tube arrangement, tube diameter, tube pitch ratio, tube length, tube number, baffle spacing ratio as well as baffle cut ratio are selected. The constraints are also introduced to ensure that the ratio of the tube length to the shell diameter is in the range of $3 < L/D_s < 12$ [2].

4.5. Gasket plate heat exchanger

Six design parameters including corrugation angle, amplitude and wavelength of chevron corrugation, plate width, plate length and the number of plates are selected for minimization of TAC in GPHE [11].

5. Optimization algorithms

In this study, four different population-based algorithms including the binary genetic algorithm (GA), real parameter genetic algorithm (RGA), particle swarm optimization (PSO) as well as differential evolutionary algorithm (DE) are used separately for optimization. In the all mentioned algorithms, a random population (or swarm in PSO) is generated. Population or swarm are consists of some chromosome (or particle in PSO) and each chromosome is formed by design parameters. After evaluation of each

chromosome using the fitness function, some operators are used to generate a new population.

A short description of these operators and constants is presented for each algorithm in the following subsections.

5.1. BGA or GA

Uniform crossover and mutation probability are employed to obtain the new population, which are shown respectively by P_c and P_m in the GA [33]. The integer-based uniform crossover operator takes two distinct parent individuals and interchanges each corresponding binary bit with a probability P_c . Moreover, the mutation operator changes each of the binary bits with a mutation probability P_m .

5.2. RGA

Such as GA, crossover and mutation are also used in RGA. Crossover operator is performed on design parameter (x) using [34]

$$x_i^{(1,t+1)} = 0.5 \left\{ (1 + \theta_i) x_i^{(1,t)} + (1 - \theta_i) x_i^{(2,t)} \right\} \quad (38)$$

and

$$x_i^{(2,t+1)} = 0.5 \left\{ (1 - \theta_i) x_i^{(1,t)} + (1 + \theta_i) x_i^{(2,t)} \right\} \quad (39)$$

where i and t indicate the i^{th} design parameter and iteration number, respectively. Moreover, θ_i is given by

$$\theta_i = \begin{cases} (2rand)^{1/(1+\eta_c)} & \text{if } rand \leq 0.5 \\ \left(\frac{1}{2-2rand} \right)^{1/(1+\eta_c)} & \text{otherwise} \end{cases} \quad (40)$$

in which, $rand$ is a random number between 0-1, and η_c is the crossover constant parameter.

The mutation operator is performed on the population as [34]

$$x_i^{(1,t+1)} = x_i^{(1,t+1)} + (x_i^{\max} - x_i^{\min}) \delta, \quad (41)$$

where δ is given by

$$\delta = \begin{cases} (2rand)^{1/(1+\eta_m)} - 1 & \text{if } rand < 0.5 \\ 1 - [2(1-rand)]^{1/(1+\eta_m)} & \text{if } rand \geq 0.5 \end{cases}, \quad (42)$$

in which, η_m is the mutation constant parameter.

5.3. The PSO

The new design parameters are obtained using the following relation in PSO [35]:

$$x_{t+1}^i = x_t^i + v_{t+1}^i, \quad (43)$$

where v_{t+1}^i is the updated velocity of each particle as obtained as bellow [35]:

$$v_{t+1}^i = wv_t^i + C_1 rand(p^i - x_t^i) + C_2 rand(p_k^g - x_t^i), \quad (44)$$

where w , C_1 and C_2 are inertia factor, self-confidence factor and swarm-confidence factor, respectively. In addition, p^i and p_k^g are the best position of each particle over time and best global value in the current swarm respectively.

5.4. DE

Mutation in *DE* is determined as [36]:

$$V_t^i = x_{t,r1}^i + F(x_{t,r2}^i - x_{t,r3}^i), \quad (45)$$

where F is differential weight factor and $x_{t,r1}^i$, $x_{t,r2}^i$ and $x_{t,r3}^i$ three random design parameters in the population for the i^{th} parameter.

Crossover in *DE* is also defined as [33]:

$$x_t^i = \begin{cases} v_t^i & \text{if } rand \leq C_r \\ x_t^i & \text{if } rand > 0.5 \end{cases}, \quad (46)$$

where C_r is crossover rate constant.

6. Results and discussion

In this study, five different heat exchangers including PFHE, FTHE, RR, STHE and GPHE are optimized using four different algorithms including GA, RGA, PSO and DE. The verified codes for the mentioned heat exchangers are used which could be found in [2, 5, 6, 10-11].

All variables and their distribution in the simulation are illustrated in Table 1. Step size and parameters range are also shown in Table 2. Each algorithm is repeated ten times for each step size. The final answer of each step is achieved by the average of solution sets.

Minimum, maximum, average and RSD of final answers are calculated and shown for each heat exchanger and algorithm in the related Tables. In this section, four algorithms including DE, GA, PSO and RGA have been implemented for each heat exchanger. TAC is considered as the objective function that should be minimized and the step size and the results of each achieved method are compared with each other according to Table 2.

Table1. algorithms parameters and their explanation

Parameter Name	Explanation
F	Differential weight in DE
Cr	Crossover rate constant in DE
Pm	Probability of mutation in GA
Pc	Probability of crossover in GA
C_1	Self-confidence factor in PSO
C_2	Swarm-confidence factor in PSO
η_M	Mutation constant parameter in RGA
η_c	Crossover constant parameter in RGA
S_F	The step size of F in DE
S_{Cr}	The step size of Cr in DE
S_{Pm}	The step size of Pm in GA
S_{Pc}	The step size of Pc GA
S_{C_1}	The step size of C_1 in PSO
S_{C_2}	The step size of C_2 in PSO
S_{η_M}	The step size of η_M in RGA
S_{η_c}	The step size of η_c RGA

Table 2. The range of parameters and their step size

Algorithm	Parameters ranges	Step size
DE	$(0 \leq F \leq 1)$, $(0 \leq Cr \leq 1)$	$S_F=0.05$, $S_{Cr}= 0.05$
GA	$(0 \leq P_m \leq 1)$, $(0 \leq P_c \leq 1)$	$S_{Pm}=0.05$, $S_{Pc}= 0.05$
PSO	$(0 \leq C_1 \leq 2.5)$, $(0 \leq C_2 \leq 2.5)$	$S_{C_1}= 0.15$, $S_{C_2}= 0.15$
RGA	$(0 \leq \eta_M \leq 4)$, $(0 \leq \eta_c \leq 4)$	$S_{\eta_M} = 0.2$, $S_{\eta_c} = 0.2$

6. 1. Numerical results for chevron (gasket) heat exchanger

Optimization results of chevron heat exchanger using four revolution algorithms are shown in Table3. By applying the DE algorithm in Chevron heat exchanger, changing in the total annual cost (TAC) versus algorithm's parameters is depicted in Fig. 2a. As it can be seen for C_r and F which are higher than 0.2, TAC tends to be the lowest amount. In the case of C_r close to zero, the algorithm leads to solutions that are far from the optimal value. Therefore, optimal solutions can be achieved for the designer according to the range close to the optimal solutions. GA algorithm is performed, and the impact of parameters changes is reported in Fig 2b. As it can be seen for $P_m < 0.5$ and $P_c < 0.1$ the total annual cost tends to be minimal. As a result, optimal solutions can be achieved in the optimal range for the designers.

It seems that the effects of parameter P_c that indicates the probability of crossover does not have much impact on the near-optimal solutions. But it should be noted that the optimal solution, in this case, can be achieved in the point $\langle P_c, P_m \rangle = (0.6, 0.05)$. In the case of Fig. 2c which is done by PSO-Chevron should be said, for c_2 less than 0.5, there has not been a good response, but by the increase of c_2 , the algorithm tends to the optimal values of the total annual cost. As it can be seen, for c_2 greater than 0.5 final solution tends to be minimal, and the best total annual cost can be achieved in the point $\langle C_1, C_2 \rangle = (0, 0.6)$. In this method of optimization, it is clear that the optimal solution does not have any dependence on the different values of C_i . For the results of RGA it can be said that nearly for all different values of η_c and η_m , the desired response is achieved as illustrated in Fig. 2d.

Table 3. Optimization results of four algorithms for Chevron heat exchanger

Chevron	Min	Mean	Max	Mean-runtime	RSD	Optimum parameters
DE	994.2126	1018.8	1432.3	13.4015	1.7772	$\langle C_r, F \rangle = (0.5, 0.4)$
GA	994.1944	1012.4	1147.7	20.5060	0.6922	$\langle P_c, P_m \rangle = (0.6, 0.05)$
PSO	994.1895	1004.4	1088.5	14.0413	0.7374	$\langle C_1, C_2 \rangle = (0, 0.6)$
RGA	994.1895	994.2	994.3	27.0738	0.0460	$\langle \eta_c, \eta_m \rangle = (2.4, 2.4)$

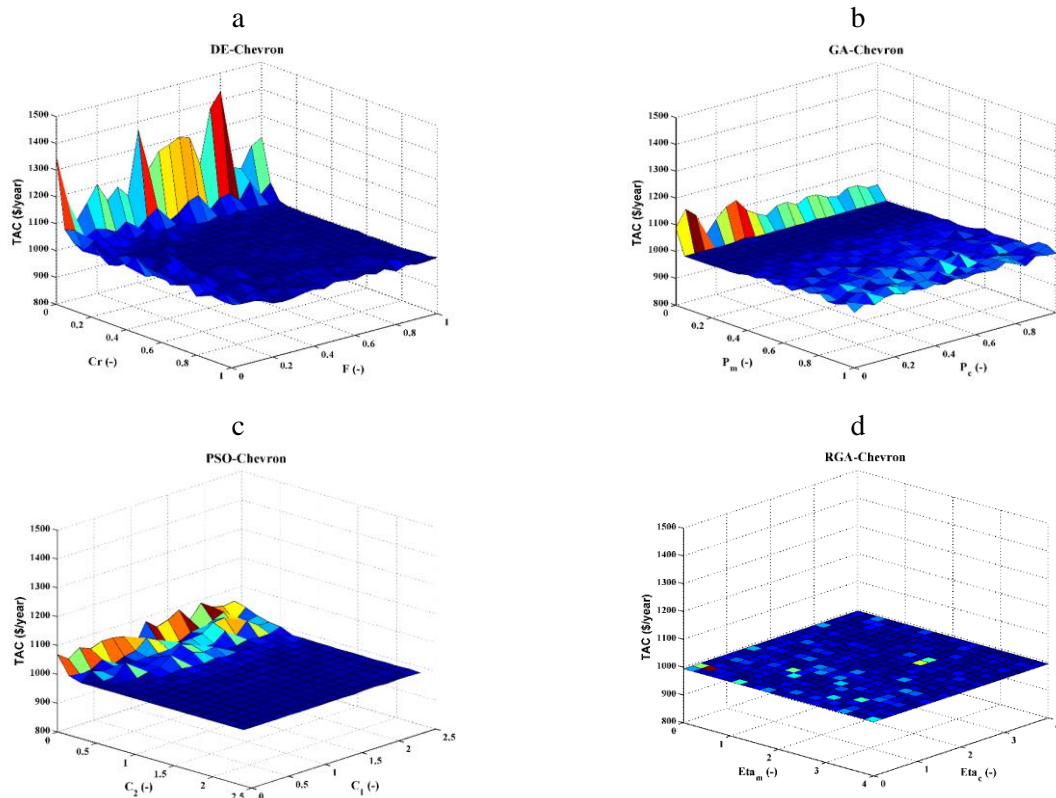


Fig. 2. Graphical results on the performance of different algorithms for Chevron Heat Exchanger for different algorithm parameters: a. Optimization of GPHE by DE, b. Optimization of GPHE by GA, c. Optimization of GPHE by PSO, d. Optimization of GPHE by RGA

6. 2. Numerical results for fin and tube heat exchanger

In the Fin Tube exchanger, algorithms are presented in terms of run time and sensitivity to input parameters (RSD) in Table 4. Optimization results of fin and tube exchangers performed by four evolutionary algorithms are given in Table 5. Optimum values obtained by four algorithms are illustrated by min. Min values obtained from all algorithms have become equal to each other by one decimal. On the other hand, maximum values are displayed for different parameters in Table 5. This indicates that a range of different solutions and thus different mean values and standard deviation can be achieved in each of these algorithms. As a result, it can be said that the PSO algorithm has the lowest run time (as shown in Table 5). In addition, parameters that lead to the best possible answers are given in Table 5 for these algorithms.

The effect of parameters' changes on the total annual cost is regular, as well as for 0.2

$\leq C_r \leq 0.8$ and F higher than 0.2 the total annual cost tends to be minimal, and in this case, the optimum solution can be achieved in the point $\langle C_r, F \rangle = (0.3, 0.7)$ as shown in Fig. 3.a. For C_r close to zero, the algorithm leads to the solutions which are far from the optimal solution as a result causes a large RSD. Optimal answers can be achieved for the design, according to the range near to the optimal solutions illustrated in Fig. 3.a. In the case of the GA algorithm, the effect of changing parameters on the final answer is also regular and can be reported. It is observed from the Fig. 3.b that for $0.1 \leq P_m \leq 0.3$ final answers tend to be minimal. As a result, answers near the optimal range should be considered in order to find the optimal solutions in the design.

It appears that the effects of parameter P_c which indicates the probability of crossover does not have much impact on the solutions close to the optimal region. But in this case, it should be noted that the optimal solution in the point $\langle P_c, P_m \rangle = (0.7, 0.05)$ is achieved. It can

be deduced that mutation has the role to change as well as evaluate the population towards the optimal solution. In the case of Fig. 3c should be said there have not been the favorable answers for C_2 less than 0.5, but by an increase in the amount of C_2 the algorithm tends towards the optimal values. As it can be seen, for C_2 more than 0.5 the total price tends to be lowest and in this case, the optimal solution happens in the point $\langle C_1, C_2 \rangle = (0, 1.95)$. This

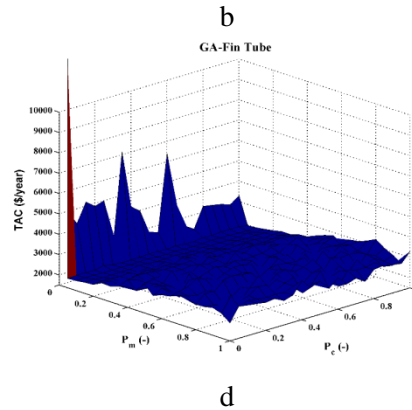
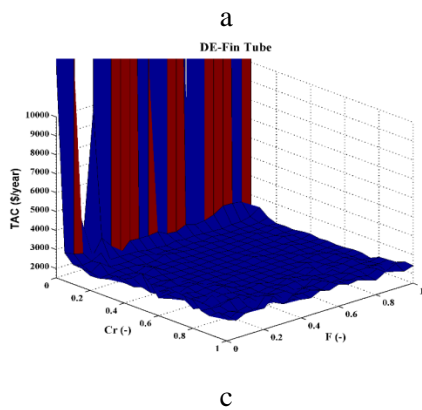
method of optimization can result that the minimum amount of price is generally independent of C_1 . In the case of the RGA algorithm should be noted that almost all the different values of η_M and η_c lead to the desired response which is shown in Fig. 3.d. As mentioned above, the obtained standard deviation in Table 5 is 0.1, which indicates that almost all the total annual costs are the same.

Table 4. Sorting algorithms based on the best runtime and RSD for different heat exchangers

Heat exchanger	Insensitivity to input parameters (RSD)	Run-Time
Chevron	RGA	DE
	GA	PSO
	PSO	GA
	DE	RGA
Fin Tube	RGA	PSO
	PSO	RGA
	DE	DE
	GA	GA
Plate Fin	RGA	PSO
	GA	DE
	PSO	RGA
	DE	GA
Regenerator	RGA	PSO
	GA	DE
	PSO	RGA
	DE	GA
Shell & Tube	RGA	PSO
	PSO	DE
	GA	RGA
	DE	GA

Table 5. Optimization results of four algorithms for Fin Tube heat exchanger

Fin Tube	Min	Mean	Max	Mean-runtime	RSD	Optimum parameters
DE	1943.4	4713.1	9581.0	108.5529	36.1995	$\langle C_r, F \rangle = (0.3, 0.7)$
GA	1947.0	3860.5	9251.3	200.8800	25.2202	$\langle P_c, P_m \rangle = (0.7, 0.05)$
PSO	1939.4	2459.1	8174.9	42.1157	14.8898	$\langle C_1, C_2 \rangle = (0, 1.95)$
RGA	1943.3	1960.2	2016.6	92.5161	0.1464	$\langle \eta_c, \eta_m \rangle = (1, 2.4)$



c

d

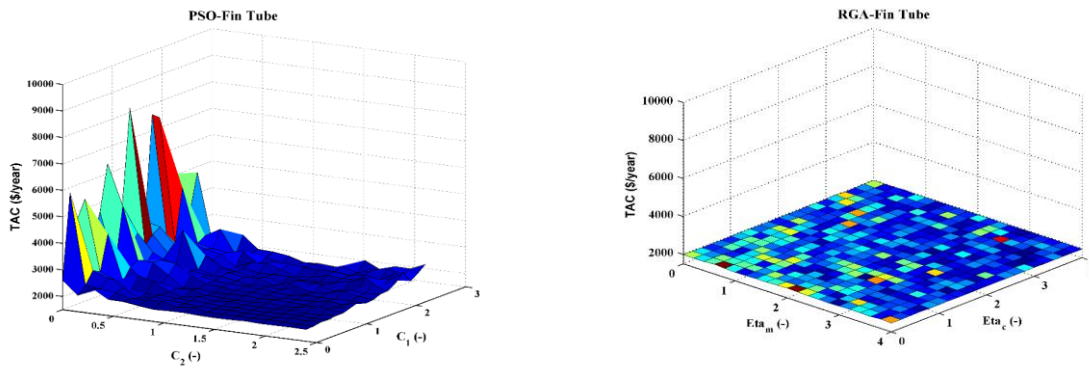


Fig. 3 Graphical results on the performance of different algorithms for Fin Tube Heat Exchanger for different algorithm parameters: a. Optimization of FTHE by DE, b. Optimization of FTHE by GA, c. Optimization of FTHE by PSO, d. Optimization of FTHE by RGA

6. 3. Numerical results for plate-fin heat exchanger

Optimization results of the plate-fin heat exchanger performed by evolutionary algorithms are listed in Table 6. The optimal values obtained by four algorithms have been shown by min and become equal to each other with two decimal place approximations. On the other hand, maximum values for some parameters are shown in this Table which indicates that a range of different solutions and thus different mean values and standard deviation can be achieved in each of these algorithms. In the mean value of RGA, solutions for different parameters, are equal to the average value with a three decimal place approximation. It is indicated that the algorithm in the case of optimization of plate-fin heat exchanger is very sensitive to how to set the parameters of the algorithm. This theme can be observed from the RSD obtained from the algorithm. For the other three algorithms, the amount of RSD differs from the RGA, but it can be said that these three algorithms provide an acceptable scattering according to the average value. But, in order to achieve the appropriate solution, evolutionary algorithm parameters should be carefully determined. PSO algorithm has the lowest runtime and is appropriate for applications where speed is the basic requirement. Algorithms applied in the plate-fin exchanger are arranged and listed in terms of runtime and sensitivity to input parameters (RSD), in Table 4. The variation of the total annual cost is shown based on the design parameters in Fig. 4a. As it can be seen for $0.05 \leq C_r \leq 0.7$, and F more than 0.2, the total cost tends to be minimal, and optimal price can be

achieved in the point $\langle C_r, F \rangle = (0.25, 0.85)$. For C_r close to zero, the total annual cost becomes far from the optimal solution and therefore causes a large RSD. For the design, the optimal price is selected according to the range near to the optimal solutions illustrated in Fig. 4a. The effect of parameters changes used in GA on the total price is also regular and can be reported the same as above. As it is clear in Fig. 4.b the total cost tends to be minimal for $0 \leq P_m \leq 0.5$. In order to find the optimal price, design parameters should be selected of the region near to the optimal situation. It seems that the effect of parameter P_c which indicates the probability of crossover does not have much impact on the solutions close to the optimal region. But in this case, it should be mentioned that the optimized total cost is achieved in the point $\langle P_c, P_m \rangle = (0.2, 0.05)$. In the case of Fig. 4c should be said for C_2 less than 0.75, a favorable price has not been obtained, but by an increase in the amount of C_2 , the algorithm tends towards the optimal values. As it can be observed for C_2 more than 1 the total price tends to be the lowest and the optimal price happens in the point $\langle C_1, C_2 \rangle = (0, 1.5)$. Therefore it can be concluded that the minimum price is generally independent of C_1 . In the case of the RGA algorithm should be noted that almost all the different values of η_m and η_c lead to an acceptable cost which is depicted in Fig. 4d. As it was mentioned in the Table, RSD is equal to 0.006 which demonstrates all the total annual costs obtained by the algorithm are nearly the same. Furthermore, the optimal value for the total cost can be achieved in the point $\langle \eta_c, \eta_m \rangle = (3.25, 3.75)$.

Table 6. Optimization results of four algorithms for Plate Fin heat exchanger

Plate Fin	Min	Mean	Max	Mean-runtime	RSD	Optimum parameters
DE	1318.5	1390.6	2679.9	89.2748	4.3120	$\langle C_r, F \rangle = (0.25, 0.85)$
GA	1314.1	1381.8	1766.4	164.9079	1.6576	$\langle P_c, P_m \rangle = (0.2, 0.05)$
PSO	1313.3	1385.9	1772.2	38.1497	2.4349	$\langle C_1, C_2 \rangle = (0, 1.5)$
RGA	1313.3	1313.7	1315.4	96.4326	0.0067	$\langle \eta_c, \eta_m \rangle = (3.25, 3.75)$

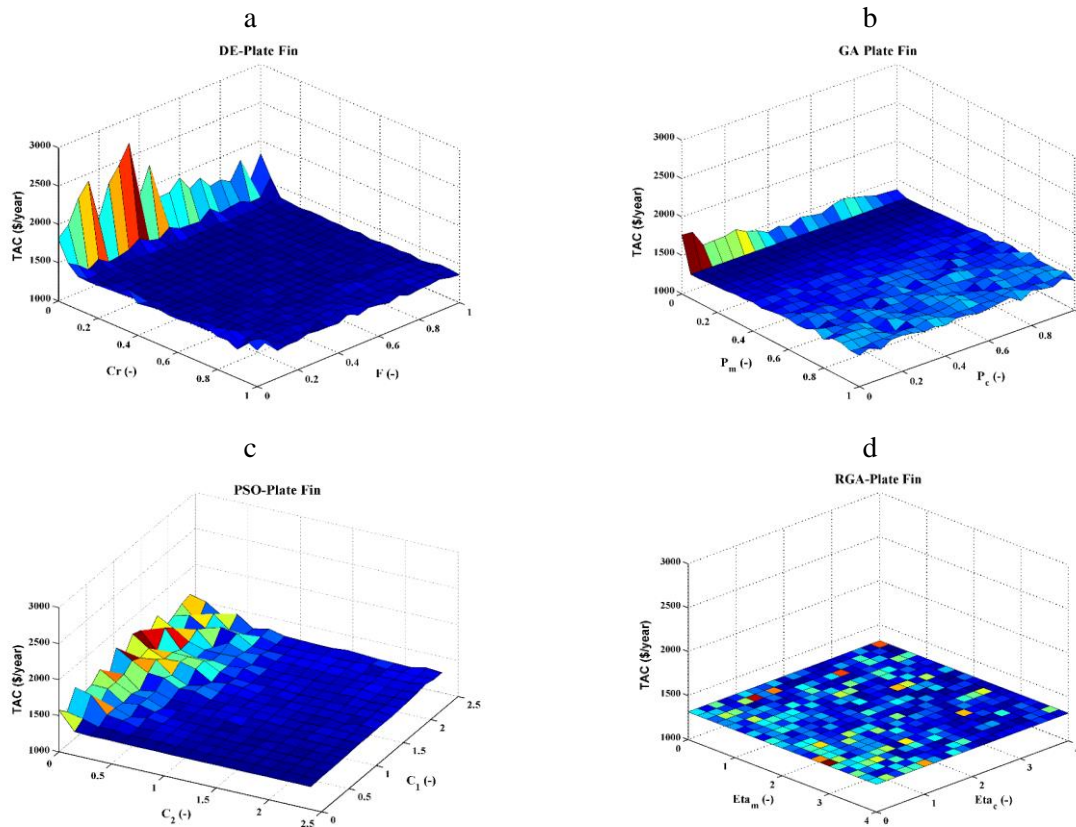


Fig. 4. Graphical results on the performance of different algorithms for Plate Fin Heat Exchanger for different algorithm parameters: a. Optimization of PFHE by DE, b. Optimization of PFHE by GA, c. Optimization of PFHE by PSO, d. Optimization of PFHE by RGA

6. 4. Numerical results for rotary regenerator

The results of Regenerator heat exchangers optimized by four evolutionary algorithms are presented in Table 7. The optimal prices obtained by four algorithms have been shown by min and become equal to each other with one decimal place approximation. Such as other analyses performed above, it is indicated that RGA is not very sensitive to how to set the parameters of the algorithm for optimization of Regenerator heat exchanger. Furthermore, Parameters that lead to the lowest price are listed in Table 7 for these algorithms. Algorithms used In the Regenerator heat exchanger are arranged and listed in terms of runtime and sensitivity to input parameters

(RSD), in Table 4. Same as above the variation of the total annual cost is shown based on the design parameters in Fig. 5a. It is demonstrated that RSD achieved in DE is larger as compared with other algorithms, but it can be said the total cost obtained for Regenerator is far away from optimal solution for $C_r < 0.3$, and optimal price can be achieved in the point $\langle C_r, F \rangle = (0.35, 0.05)$. In Fig. 5.b for $0.1 \leq P_m \leq 0.8$ the total cost tends to be optimized. In this case, the optimized total cost is achieved in the point $\langle P_c, P_m \rangle = (0.85, 0.05)$. In the case of Fig. 5.c it should be said for C_2 less than 1, a reasonable result has not been obtained, but by an increase in the amount of C_2 , the algorithm tends towards the optimal values. As it can be observed, for C_2 more than 1 the total price tends

Table 7. Optimization results of four algorithms for rotary regenerator heat exchanger

Regenerator	Min	Mean	Max	Mean-Runtime	RSD	Optimum parameters
DE	1692.6	1777.1	2124.4	26.3049	0.7346	$\langle C_r, F \rangle = (0.35, 0.05)$
GA	1678.6	1709.8	1930.6	85.1143	0.6064	$\langle P_c, P_m \rangle = (0.85, 0.05)$
PSO	1678.1	1719.4	1856.2	22.9985	0.6599	$\langle C_1, C_2 \rangle = (0, 2.1)$
RGA	1678.1	1678.4	1681.0	54.4206	0.0075	$\langle \eta_c, \eta_m \rangle = (3.15, 3)$

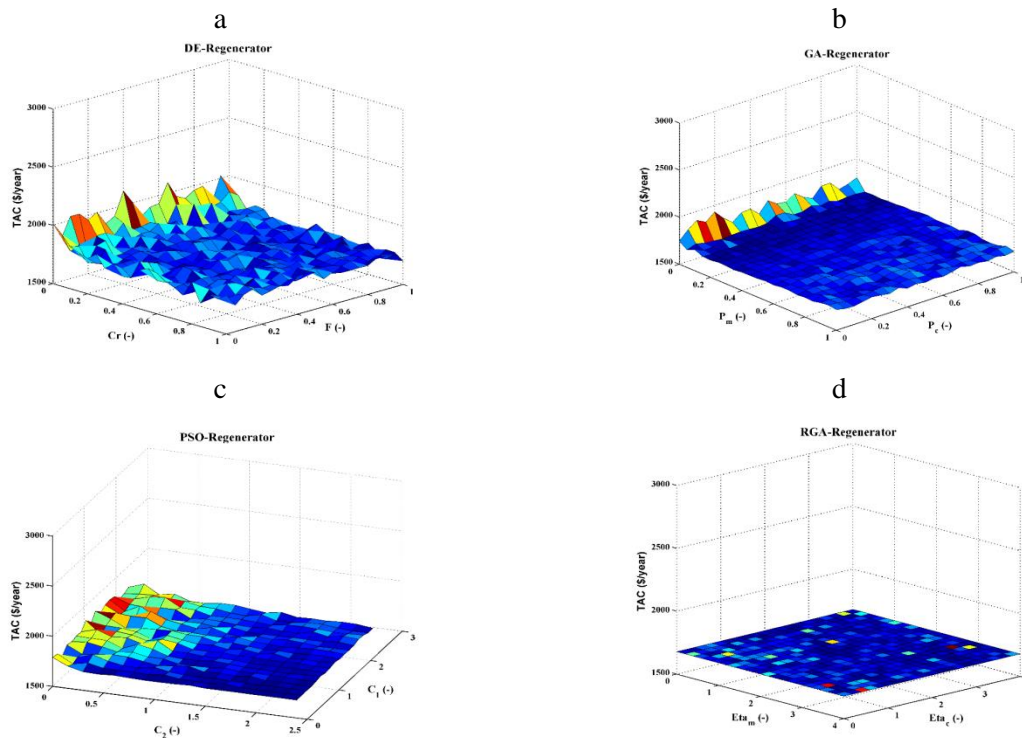


Fig. 5. Graphical results on the performance of different algorithms for Rotary Regenerator for different algorithm parameters: a. Optimization of RR by DE, b. Optimization of RR by GA, c. Optimization of RR by PSO, d. Optimization of RR by RGA

to be the lowest and the optimal price happens in the point $\langle C_1, C_2 \rangle = (0, 2.1)$. Therefore it can be inferred that the minimum price is generally independent of C_1 . As it is shown in the Table, RSD is approximately 0.007 which displays all the total annual costs obtained by the algorithm are nearly equal. Furthermore, the optimal value for the total cost is achieved in the point $\langle \eta_c, \eta_m \rangle = (3.15, 3)$

6. 5. Numerical results for shell and tube heat exchanger

Optimization results of shell and tube exchangers optimized by four evolutionary algorithms are given in Table 8. The optimal values obtained by four algorithms have been shown by min and become equal to each other with one decimal place approximation. Such as other simulations, maximum values for

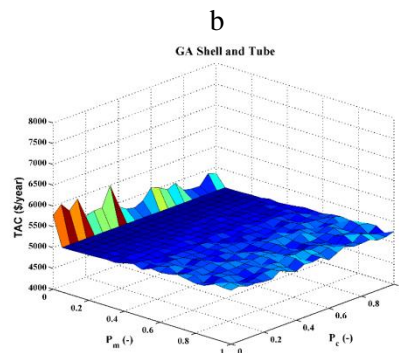
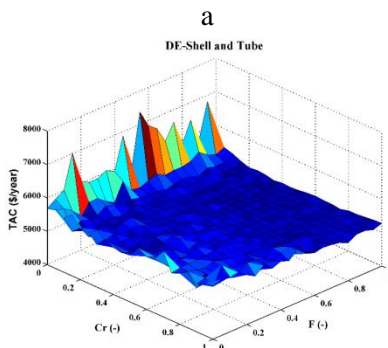
some parameter values are shown in Table 8 which indicates that in each of these algorithms, a range of different solutions and thus different mean values and standard deviation, can be achieved. In the mean value of algorithm RGA, solutions for different parameters, are equal to the average value with one decimal place approximation. It is indicated that the algorithm for optimization of shell and tube exchanger is not very sensitive to how to set the parameters of the algorithm. This result can be proved by the amount of RSD obtained for the algorithm. In three other algorithms, the amount of RSD obtained with respect to the mean value is acceptable. But, in order to achieve an appropriate response, evolutionary algorithm parameters should be carefully defined. Since the PSO algorithm has the lowest runtime,

these algorithms are essential in applications where speed is the basic requirement. Parameters that lead to the best possible answers are listed in Table 8 for these algorithms. Algorithms used In the Shell and Tube exchanger are arranged and listed in terms of runtime and sensitivity to input parameters (RSD), in Table 4. The variation of the total annual cost based on the algorithm parameters is shown In Fig. 6. Parameters changes on the final solutions are regular in the Fig. 6.a, as it can be seen algorithm tends to minimize the total annual cost for $0.2 \leq C_r \leq 0.9$ and F more than 0.2, and optimal solution can be achieved in the point $\langle C_r, F \rangle = (0.3, 0.9)$. In the case of $C_r < 0.2$, it should be said that the algorithm leads to the solutions that are far from the optimal solution, and causes an RSD greater than other algorithms. According to the range near to the optimal solutions, the best answer can be achieved. The effects of parameter changes on the final price are regular and reported in Fig. 6.b. As it can be observed for $0 < P_m \leq 0.7$ the total cost tends towards the minimum price. It seems that the effects of parameter P_c that indicates the probability of crossover does not have

much influence on the price close to the optimal cost. But it should be noted that the optimal price can be achieved in the point $\langle P_c, P_m \rangle = (0.85, 0.1)$. In Fig. 6.c for $C_2 < 0.7$, the favorable solutions are not achieved but by an increase of C_2 , optimum values for the total annual cost would be attained. For $C_2 \geq 0.7$ the total annual cost tends to be optimized and the optimal solution is achieved in the point $\langle C_1, C_2 \rangle = (0, 1.65)$. As a result, the total annual cost of shell and tube heat exchanger optimized by this method is independent of C_1 . It can be concluded from Fig. 6.d that desired total cost is achieved for all different values of parameters η_c and η_m . As it was seen in Table 8, RSD is approximately obtained 0.01 which proves the equality of all prices. The optimal value for the total cost can be achieved in the point $\langle \eta_c, \eta_m \rangle = (2.6, 2.8)$. In the end, the results of different algorithms on the particular heat exchangers in order to find the best and optimal solutions are compared to each other in Fig. 7. As it can be observed RGA algorithm is the best in order to reach the minimal TAC, and PSO, GA and DE are in the next rankings.

Table 8. Optimization results of four algorithms for Shell and Tube heat exchanger

Shell & Tube	Min	Mean	Max	Mean-runtime	RSD	Optimum parameters
DE	5066.3	5315.6	7369.5	26.6997	1.6392	$\langle C_r, F \rangle = (0.3, 0.9)$
GA	5044.7	5186.5	5994.0	51.2938	1.0032	$\langle P_c, P_m \rangle = (0.85, 0.1)$
PSO	5037.8	5150.5	5663.0	25.2762	0.6859	$\langle C_1, C_2 \rangle = (0, 1.65)$
RGA	5038.9	5045.1	5065.0	36.4988	0.0179	$\langle \eta_c, \eta_m \rangle = (2.6, 2.8)$



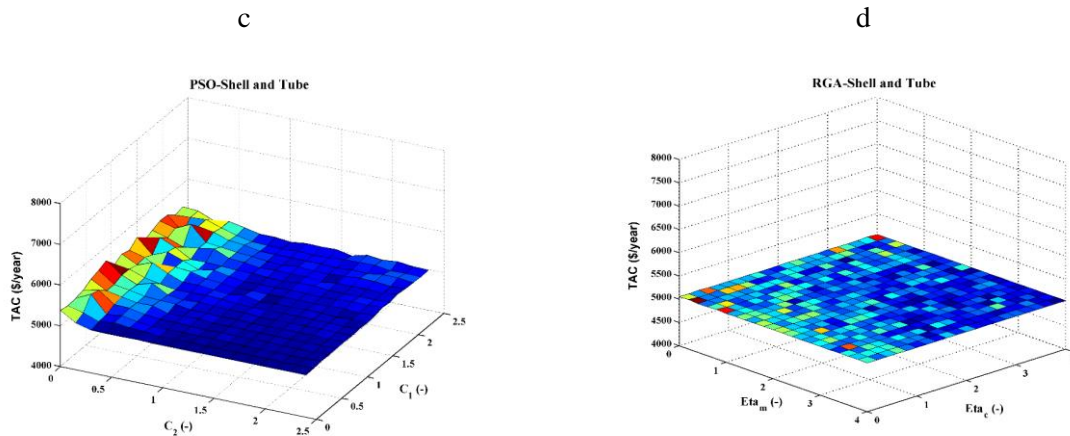


Fig. 6. Graphical results on the performance of different algorithms for Shell and Tube Heat Exchanger for different algorithm parameters: a. Optimization of STHE by DE, b. Optimization of STHE by GA, c. Optimization of STHE by PSO, d. Optimization of STHE by RGA

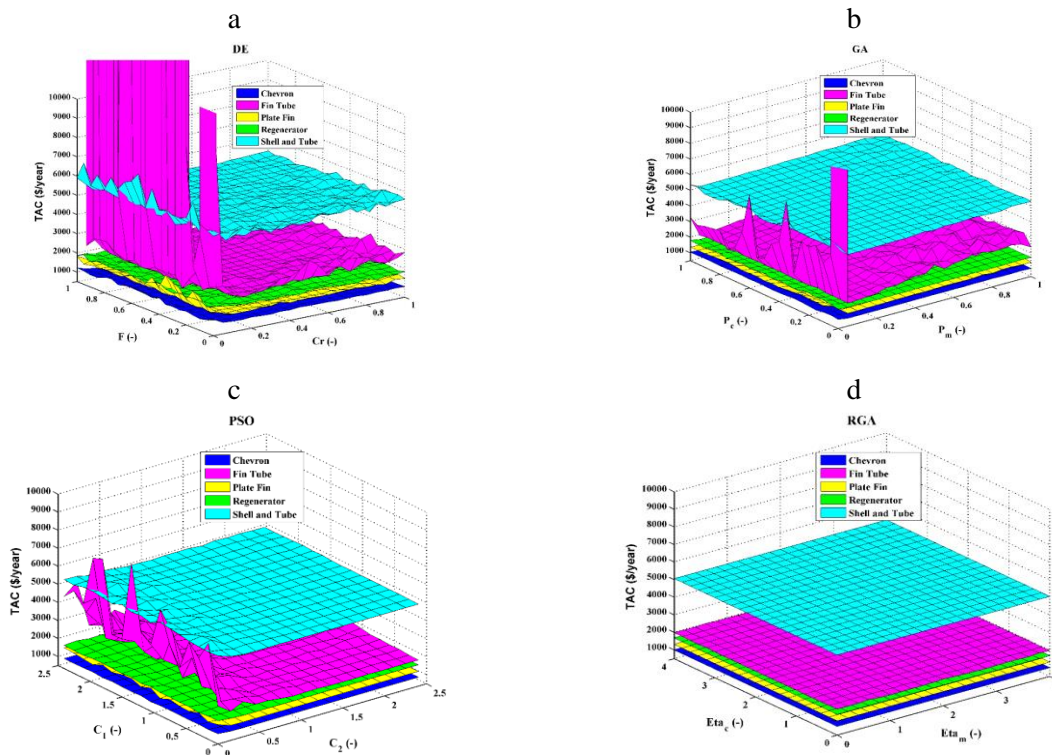


Fig. 7. Comparison of the solutions for different algorithms in the particular heat exchangers a. DE, b. GA, c. PSO, d. RGA

7. Conclusion

In this study, five different heat exchangers including PFHE, FTHE, RR, STHE and GPHE were optimized using four different algorithms including GA, RGA, PSO and DE. All the algorithms applied to the heat exchangers were also investigated in the viewpoint of run-time and insensitivity to the input parameters (RSD). TAC was considered as the objective function,

and the configuration parameters for each heat exchanger were chosen as design parameters, and following results were inferred:

- By applying RGA, the lowest RSD could be obtained for the optimization purpose, and PSO, GA and DE were in the next rankings. Therefore, RGA is a suitable choice, where the lowest RSD is our basic requirement.

- The lowest run-time was achieved, when PSO was implemented in the modeling, and DE, RGA and GA were in the next rankings. Therefore, PSO is a suitable choice, where speed is our basic requirement.
- The best results for optimization of TAC were established by using RGA in all heat exchangers, and PSO, GA and DE were in the next rankings.
- The best total annual cost in the chevron heat exchanger can be achieved in the points $\langle C_1, C_2 \rangle = (0, 0.6)$ and $\langle \eta_c, \eta_m \rangle = (2.4, 2.4)$ where the lowest run-time and RSD are our basic requirements, respectively
- The best total annual cost in the fin and tube heat exchanger can be achieved in the points $\langle C_1, C_2 \rangle = (0, 1.95)$ and $\langle \eta_c, \eta_m \rangle = (1, 2.4)$ where the run-time and RSD are our basic requirements, respectively.
- The best total annual cost in the plate-fin heat exchanger can be achieved in the points $\langle C_1, C_2 \rangle = (0, 1.5)$ and $\langle \eta_c, \eta_m \rangle = (3.25, 3.75)$ where the run-time and RSD are our basic requirements, respectively.
- The best total annual cost in the rotary regenerator can be achieved in the points $\langle C_1, C_2 \rangle = (0, 2.1)$ and $\langle \eta_c, \eta_m \rangle = (3.15, 3)$ where the run-time and RSD are our basic requirements, respectively.
- The best total annual cost in the shell and tube heat exchanger can be achieved in the points $\langle C_1, C_2 \rangle = (0, 1.65)$ and $\langle \eta_c, \eta_m \rangle = (2.6, 2.8)$ where the run-time and RSD are our basic requirements, respectively.

Replication of results

results are presented

Conflict of interest

On behalf of all authors, the corresponding author states that there is no conflict of interest.

Data Availability

The data will be made available on request

References

- [1] Hassan. Hajabdollahi, Pouria Ahmadi, Ibrahim Dincer. Exergetic optimization of shell-and-tube heat exchangers using NSGA-II. *Heat Transfer Engineering* 33 (2012) 618-628.
- [2] Sepehr. Sanaye, Hassan. Hajabdollahi, Multi-objective optimization of shell and tube heat exchangers, *Applied Thermal Engineering* 30 (2010) 1937-1945.
- [3] Rihanna Khosravi, Abbas Khosravi, Saeid Nahavandi, Hassan Hajabdollahi, Effectiveness of evolutionary algorithms for optimization of heat exchangers, *Energy Conversion and Management*, 89, (2015), 281-288
- [4] Hassan. Hajabdollahi, Pouria Ahmadi, Ibrahim Dincer, Thermoeconomic optimization of a shell and tube condenser using the evolutionary algorithm", *International Journal of Refrigeration*, 34 (2011), 1066-1076.
- [5] Sepehr Sanaye, Hassan Hajabdollahi, Thermal-Economic Multi-objective Optimization of Plate Fin Heat Exchanger Using Genetic Algorithm, *Applied Energy*, 87 (2010), 1893–1902.
- [6] Pouria Ahmadi, Hassan Hajabdollahi and Ibrahim Dincer, "Cost and Entropy generation minimization of a cross-flow Plate-Fin Heat Exchanger (PFHE) using Multi-Objective genetic algorithm" *ASME Transaction, Journal of Heat Transfer*, 133 (2010) 021801.
- [7] Hassan. Hajabdollahi, Mojtaba Tahani , M.H. shojaee fard. CFD modeling and multiobjective optimization of compact heat exchanger using CAN method, *Applied Thermal Engineering* 31 (2011) 2597-2604.
- [8] Hassan Hajabdollahi, Pouria Ahmadi, Ibrahim Dincer "Modeling and Multi-Objective Optimization of Plain Fin and Tube Heat Exchanger Using Evolutionary Algorithm" *International Journal of Thermophysics and Heat Transfer* 3 (2011) 424-431.
- [9] Amir hesan kashani nia, mohammad madahi, Hassan. Hajabdollahi, Thermoeconomic optimization of Air-cooled heat exchanger. *Applied thermal engineering* 54 (2013) 43-55.

- [10] Sepehr. Sanaye, Hassan. Hajabdollahi, Multi-objective optimization of rotary regenerator using genetic algorithm, *International Journal of Thermal Sciences*, 48 (2009) 1967–1977.
- [11] Farzaneh. Hajabdollahi, Zahra Hajabdollahi, Hassan Hajabdollahi. Optimum Design of Gasket Plate Heat Exchanger Using Multimodal Genetic Algorithm. *Heat Transfer Research* 44 (2013).
- [12] H. Sadeghzadeh, M.A. Ehyaei, M.A. Rose, Techno-economic optimization of a shell and tube heat exchanger by genetic and particle swarm algorithms, *Energy Conversion and Management*, 93 (2015) 84–91.
- [13] H. Sadeghzadeh, M. Aliehyaei, MA. Rosen. "Optimization of a Finned Shell and Tube Heat Exchanger Using a Multi-Objective Optimization Genetic Algorithm." *Sustainability* 7, no. 9 (2015): 11679-11695.
- [14] B.V. Babu, S.A. Munawar, Differential evolution strategies for the optimal design of shell-and-tube heat exchangers, *Chemical Engineering Science*, 62 (2007) 3720-3739.
- [15] H. Hajabdollahi, Investigating the effect of non-similar fins in thermo-economic optimization of plate-fin heat exchanger, *Applied Thermal Engineering*, 82 (2015) 152-161.
- [16] O. Emrah Turgut, Hybrid Chaotic Quantum behaved Particle Swarm Optimization algorithm for thermal design of plate fin heat exchangers, *Applied Mathematical Modelling*, In Press, Corrected Proof, Available online 4 June 2015
- [17] OE. Turgut, MS. Turgut, MT. Coban. "Design and economic investigation of shell and tube heat exchangers using Improved Intelligent Tuned Harmony Search algorithm." *Ain Shams Engineering Journal* 5, no. 4 (2014): 1215-1231.
- [18] Z. Wang, Y. Li, Irreversibility analysis for optimization design of plate fin heat exchangers using a multi-objective cuckoo search algorithm, *Energy Conversion and Management*, 101 (2015): 126-135.
- [19] J. Lee, K.-Soo Lee., Friction and Colburn factor correlations and shape optimization of chevron-type plate heat exchangers, *Applied Thermal Engineering*, 89 (2015) 62-69.
- [20] M.A. Arie, A.H. Shooshtari, S.V. Dessiatoun, E. Al-Hajri, M.M. Ohadi, Numerical modeling and thermal optimization of a single-phase flow manifold-microchannel plate heat exchanger, *International Journal of Heat and Mass Transfer*, 81 (2015) 478-489.
- [21] S.W. Hong, S.H. Ahn, O.K. Kwon, J.D. Chung, Optimization of a fin-tube type adsorption chiller by the design of experiment, *International Journal of Refrigeration*, 49 (2015) 49-56.
- [22] Kubo, S., Yaji, K., Yamada, T. *et al.* A level set-based topology optimization method for optimal manifold designs with flow uniformity in plate-type microchannel reactors. *Struct Multidisc Optim* 55, 1311–1327 (2017).
- [23] Ramalingom, D., Cocquet, P., Maleck, R. *et al.* A multi-objective optimization problem in mixed and natural convection for a vertical channel asymmetrically heated. *Struct Multidisc Optim* 60, 2001–2020 (2019).
- [24] Jinyang Wang, Guomin Cui, Yuan Xiao, Xing Luo & Stephan Kabelac (2017) Bi-level heat exchanger network synthesis with evolution method for structure optimization and memetic particle swarm optimization for parameter optimization, *Engineering Optimization*, 49:3, 401-416.
- [25] Hajabdollahi, H., Ahmadi, P., & Dincer, I. (2011). Multi-objective optimization of plain fin-and-tube heat exchanger using evolutionary algorithm. *Journal of thermophysics and heat transfer*, 25(3), 424-431.
- [26] Ahmadi, P., Hajabdollahi, H., & Dincer, I. (2011). Cost and entropy generation minimization of a cross-flow plate fin heat exchanger using multi-objective genetic algorithm. *Journal of heat transfer*, 133(2).
- [27] Hajabdollahi, H., Ahmadi, P., & Dincer, I. (2011). Thermoeconomic optimization of a shell and tube condenser using both genetic

- algorithm and particle swarm. *International journal of refrigeration*, 34(4), 1066-1076.
- [28] R.K. Shah, P. Sekulic, *Fundamental of Heat Exchanger Design*. John Wiley & Sons, Inc, 2003.
- [29] R.M. Manglik, A.E. Bergles, Heat transfer and pressure drop correlations for the rectangular offset-strip-fin compact heat exchanger, *Exp. Therm. Fluid Sci.* 10 (1995) 171–180.
- [30] Wang, C. C., Chi, K. U., and Chang, C. J., "Heat Transfer and Friction Characteristics of Plain Fin-and-Tube Heat Exchanger, Part 2: Correlation," *International Journal of Heat and Mass Transfer*, 43 (2000) 2693–2700.
- [31] Hajabdollahi, Farzaneh, Zahra Hajabdollahi, and Hassan Hajabdollahi. "Thermo-economic modeling and optimization of underfloor heating using evolutionary algorithms." *Energy and Buildings* 47 (2012): 91-97.
- [32] Sunders, E. A. D., *Heat Exchangers: Selection Design and Construction*, New York: Wiley.
- [33] Goldberg, David E., and John H. Holland. "Genetic algorithms and machine learning." *Machine learning* 3.2 (1988): 95-99.
- [34] Deb K. *Multi-objective optimization using evolutionary algorithms*. Chichester: John Wiley and Sons, Ltd.; 2001.
- [35] J. Kennedy, R. Eberhart, *Particle Swarm Optimization*, Proceedings of the IEEE International Conference on Neural Networks, Perth, Australia, (1995) 1942–1945.
- [36] Storn, Rainer, and Kenneth Price. "Differential evolution—a simple and efficient heuristic for global optimization over continuous spaces." *Journal of global optimization* 11.4 (1997): 341-359.